TASK QUARTERLY 6 No 1 (2002), 127–142

MODERN FINITE VOLUME METHODS SOLVING INTERNAL FLOW PROBLEMS

KAREL KOZEL AND JAROSLAV FOŘT

Department of Technical Mathematics, CTU Prague,
Karlovo náměstí 13, 121 35 Praha 2, Czech Republic
kozelk@fsik.cvut.cz, fort@marian.fsik.cvut.cz

(Received 25 June 2001; revised manuscript received 10 August 2001)

Abstract: The paper deals with explicit and implicit finite difference and mainly finite volume schemes that have been commonly used in last years for compressible and incompressible fluid flow problems. Mainly we mention schemes used for transonic flow computation (inviscid as well as viscous models) in internal and also external aerodynamics. We prefer modern schemes like RK multistage schemes, TVD and ENO schemes, implicit schemes or higher order schemes.

Some results of numerical computation or numerical simulation are presented in the second part of the paper, including 2D and 3D transonic flow through a channel and a cascade (mainly of turbine type), 2D and 3D backward facing step flow (laminar and turbulent), 2D and 3D impinging jet flow (comparisons of some turbulent models). The last two cases have been computed only for incompressible viscous flows. Some tests for the efficiency of higher order scheme (4^{th}–6^{th} order) are presented for the backward facing step problem.

In many examples we also present a comparison of numerical and experimental results.

Keywords: finite volumes, modern numerical schemes, internal aerodynamics

1. Introduction

Since 1970 we can observe fast progress in numerical solution of transonic flows in external and internal aerodynamics. Allow us to mention first two methods published in 1969 and 1971. The first one was the method of Murman and Cole [1] based on numerical solution of the small disturbance potential equation and the second one was the method of Magnus and Yoshihara [2] solving numerically the system of Euler equations. These two original methods were the starting point of a new period in development of numerical methods and successful computation of inviscid and viscous transonic flow. Mainly the second method initiated (with development of computers) a fast progress in numerical analysis and construction of new schemes, which have been used for numerical simulations of important engineering and physical problems in external and internal aerodynamics.

Transonic flow (2D cascades) was first solved in the Czechoslovak Republic by some extension of the Murman-Cole method. The model of the small disturbance potential equation was solved in a non-orthogonal grid by a second order finite difference non-conservative method and later by a finite-volume conservative method [3, 4].

Then we extended the method for the full potential equation in 2D. The achieved results and their comparison with experiments show suitable properties of the developed methods. Figure 1 shows measured and computed results of transonic flows through a DCA 8% cascade. The measurements carried out at IT CAS – Figure 1a. The numerical method was developed at CTU Prague (small disturbance potential equation) – Figure 1b. The last picture (Figure 1c) shows results of Akay, Eccer (USA), computed by the finite element method for the full potential equation, achieved in 1981. The agreement between the experiment and numerical solution (Figure 1a, b) validated the fact that flow through the DCA 8% cascade is realized also for slightly higher M_∞ than M_∞^c, where M_∞^c denotes the lowest value of inlet Mach number for which the sonic line closes the blade channel. Figure 2 shows results of transonic flow ($M_\infty < 1$) through a compressor cascade of the ČKD Compressors factory (computed choked flows – with the full potential equation). Later we developed several methods to solve the system of Euler and Navier-Stokes equations.

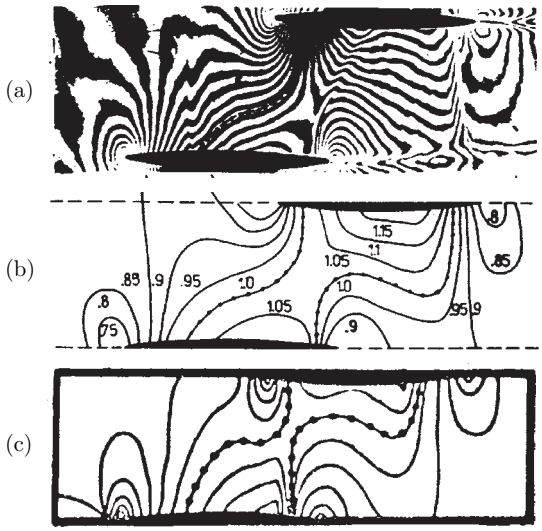

Figure 1. Transonic flow in DCA 8% cascade of IT CAS, measured and computed results

2. Mathematical models

Generally speaking compressible flows could be described by an inviscid isentropic model (small disturbance or full potential equation), the system of Euler equations (inviscid model) and system of Navier-Stokes equations. All the mentioned mathematical models can be written in nonconservative and also in conservative forms. An incompressible viscous flow is described by the system of Navier-Stokes equations. In many cases one does not use the full system of Navier-Stokes equations, but other models derived from this system, *e.g.* models based on the stream function and potential function, or stream function and vorticity or momentum equations and Poisson equation for pressure. We also have a chance to use several mathematical modifications of the system of Navier-Stokes equations in 2D and 3D, *e.g.* artificial compressibility, dual time stepping. In some cases these modifications could reduce

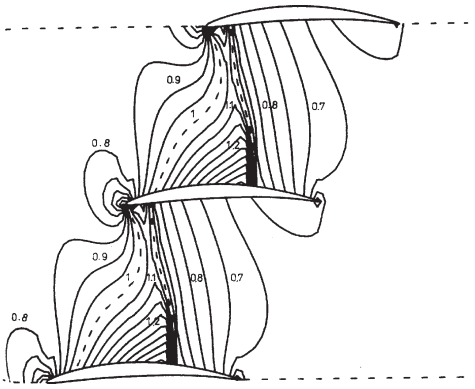

Figure 2. Compressor cascade of ČKD compressors Ltd. Prague; computation of chocked flow (full potential equation)

the number of unknowns or help in construction of an efficient method – used grid, numerical algorithm.

2.1. 2D governing equations

Let us consider the following system of governing equations.

a) The small disturbance potential equation in nonconservative form:

$$(K_1 - K_2\varphi_x)\varphi_{xx} + \varphi_{\tilde{y}\tilde{y}} = 0, \quad \tilde{y} = \delta^{2/3} y, \quad K_1 > 0, \quad K_2 > 0 \tag{1}$$

or in conservative form

$$(K_1\varphi_x - K_2\varphi_x^2)_x + (\varphi_{\tilde{y}})_{\tilde{y}} = 0 \quad K_i = K_i(M_\infty, \delta), \quad i = 1,2, \tag{2}$$

where the unknown variable φ is the potential of the disturbed velocity.

b) The full potential equation in nonconservative form

$$(a^2 - \Phi_x^2)\Phi_{xx} + 2\Phi_x\Phi_y\Phi_{xy} + (a^2 - \Phi_y^2)\Phi_{yy}, \quad a^2 = a^2(\Phi_x^2 + \Phi_y^2) \tag{3}$$

or conservative form

$$(\rho\Phi_x)_x + (\rho\Phi_y)_y = 0, \quad \rho = \rho(\Phi_x^2 + \Phi_y^2), \tag{4}$$

where the unknown variable Φ is the velocity potential, ρ is the density.

c) The system of Euler equations in conservative form

$$\mathbf{W}_t + \mathbf{F}_x + \mathbf{G}_y = 0, \tag{5}$$

where $\mathbf{W} = [\rho, \rho u, \rho v, e]^T$ are conservative variables and $\mathbf{F} = [\rho u, \rho u^2 + p, \rho uv, u(e+p)]^T$, $\mathbf{G} = [\rho v, \rho vu, \rho v^2 + p, , v(e+p)]^T$ are physical fluxes (inviscid).

d) The system of Navier-Stokes equations in conservative form

$$\mathbf{W}_t + \mathbf{F}_x + \mathbf{G}_y = \mathbf{R}_x + \mathbf{S}_y, \tag{6}$$

where $\mathbf{R} = [0, \tau_{xx}, \tau_{xy}, u\tau_{xx} + v\tau_{xy} + kT_x]^T$, $\mathbf{S} = [0, \tau_{xy}, \tau_{yy}, u\tau_{xy} + v\tau_{yy} + kT_y]^T$, $\tau_{xx} = \mu(4/3u_x - 2/3v_y)$, $\tau_{xy} = \mu(u_y + v_x)$, $\tau_{yy} = \mu(-2/3u_x + 4/3v_y)$, μ is viscosity coefficient, $\mathbf{R}$, $\mathbf{S}$ are so-called viscous physical fluxes.

All 2D equations are commonly used for computation, the system of Navier-Stokes Equations (6) describes the so-called laminar flow. The Navier-Stokes equations for incompressible flows have the following form

$$\tilde{R}\mathbf{W}+\mathbf{F}_x+\mathbf{G}_y=\nu(\mathbf{R}_x+\mathbf{S}_y), \tag{7}$$

where $\mathbf{W}=[p,u,v]^T$, $\mathbf{F}=[u,u^2+p,uv]^T$, $\mathbf{G}=[v,uv,v^2+p]^T$, $\mathbf{R}=[0,u_x,v_x]^T$, $\mathbf{S}=[0,u_y,v_y]^T$, $\nu=\mu/\rho_0$, $p=P/\rho_0$, P denotes pressure and ρ_0 is density (constant), $\tilde{R}=diag(0,1,1)$.

2.2. Boundary conditions

Formulation of boundary conditions for the potential equation is relatively clear (*e.g.* we have a mixed boundary value problem for one partial differential equation of second order in the case of subsonic flow near inlet and outlet boundaries). Upstream boundary conditions for Euler equations, where $M_{\infty,n}$ (Mach number of upstream normal velocity component) is subsonic in 2D, are considered in a form of three conditions for the components of $\mathbf{W}$. For the downstream part of the boundary with $M_{2,n}<1$, one condition (*e.g.* pressure) is given. When $M_{\infty,n}>1$, all 4 components are given and for $M_{2,n}>1$ no boundary condition is prescribed. On the wall, for the case of Euler equations $\rho q_n=0$, where q_n is the component of vector $(u,v)^T$ normal to the boundary (wall). Non-slip boundary conditions on the walls are considered, temperature T is given or $\partial T/\partial n=0$ on the wall for the case of Navier-Stokes equations. The numerical method usually extrapolates some variables to complete the conditions for unknown components of $\mathbf{W}$ at the corresponding boundary.

3. Numerical solution

Numerical methods based on the potential model are not frequently published last time, mainly Euler equations or Navier-Stokes equations (laminar or RANS) are used as the basic mathematical models. Three traditional methods are used for solving CFD problems: finite difference method, finite volume method and finite element method. For transonic flow problems, the first two methods are most popular, finite element method is not frequently used, but the method is in fast progress (discontinuous Galerkin method [5, 6]) at this time.

One of the main concerns of numerical solution of Euler or Navier-Stokes equations seems to be an approximation of the convective terms. It necessarily

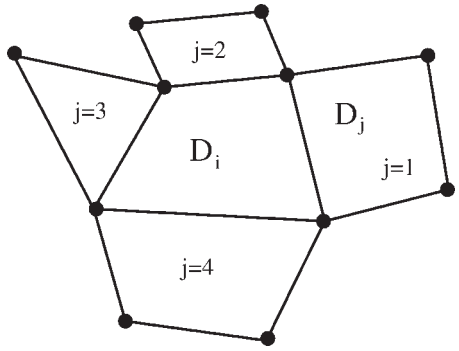

Figure 3. Finite volume D_i and neighbour volumes D_j, $j=1,\ldots,n$

has a part called artificial viscosity term that is included in upwind schemes or added in central schemes. The other important concern is choice of grid (structured, unstructured, adaptive, ...) or multi-grid method, used mainly for steady state problems, to achieve fast convergence. Mesh can very much influence numerical results, and adaptivity of the grid during the solution can improve the results of numerical simulation. The type of finite volume method is very important for numerical approximation of boundary conditions in connection with the scheme and grid (cell centered, cell vertex, cell edged, dual finite volumes or its combination used at quadrilateral grid, triangular, ...). Similar is also true for turbulence models and RANS (Reynolds Averaged Navier-Stokes) equations.

Consider the finite volume method now. The domain of solution is divided into small subdomains D_i, where $\bigcup_i D_i = D$ and $D_j \cap D_i = 0$, see Figure 3.

Then in the cell centered form ($\mathbf{W}_i$ is mean value of $\mathbf{W}$ in D_i) we have after integration of (6) over D_i and using the mean value theorem and Green's theorem

$$\mathbf{W}_i^{n+1} = \mathbf{W}_i^n - \frac{\Delta t}{\mu_i}\left(\oint_{\partial D_i} \mathbf{F}dy - \mathbf{G}dx + \oint_{\partial D_i} \mathbf{R}dy - \mathbf{S}dx\right), \quad \mu_i = \int\int_{D_i} dx\,dy. \tag{8}$$

In the numerical scheme we fulfill

$$\mathbf{W}_i^{n+1} = \mathbf{W}_i^n - \frac{\Delta t}{\mu_i}\sum_{k=1}^{N}(\tilde{\mathbf{F}}_k - \tilde{\mathbf{R}}_k)\Delta y_k - (\tilde{\mathbf{G}}_k - \tilde{\mathbf{S}}_k)\Delta x_k, \tag{9}$$

where $\tilde{\mathbf{F}}_k$ is the numerical flux (approximation of the physical flux), and similarly for $\tilde{\mathbf{G}}_k$, $\tilde{\mathbf{R}}_k$, $\tilde{\mathbf{S}}_k$. Terms $\tilde{\mathbf{F}}_k$, $\tilde{\mathbf{G}}_k$ are inviscid and $\tilde{\mathbf{R}}_k$, $\tilde{\mathbf{S}}_k$ are viscous fluxes.

Only central schemes (central differences) are commonly used for approximation of dissipative terms. Therefore we deal more with an approximation of convective terms. When we want to explain some ideas how to construct a numerical scheme in most multi-dimensional cases, we start with a 1D nonlinear scalar model of Euler equations (Cauchy problem)

$$\begin{aligned} u_t + f(u)_x &= 0 \qquad x \in (-\infty,\infty), \quad t > 0 \\ u(x,0) &= u_0(x) \end{aligned} \tag{10}$$

One can consider the scheme (conservative) in the form

$$u_k^{n+1} = u_k^n - \frac{\Delta t}{\Delta x}(\tilde{f}_{k+1/2} - \tilde{f}_{k-1/2}), \tag{11}$$

where $\tilde{f}$ is the numerical flux as some approximation of the physical flux f in (10). The consistency of the scheme (11) is fulfilled if

$$\tilde{f}_{k+1/2}(u,u,\ldots,u) = f(u). \tag{12}$$

In most cases one can express

$$\tilde{f}_{k+1/2} = \frac{1}{2}(f_{k+1} + f_k) + \frac{1}{2}Q_{k+1/2}(u_{k+1} - u_k), \tag{13}$$

where Q does not decrease the order of consistency and depends on u and derivatives of u (expressed in a numerical way). In the term Q one can imagine *e.g.* some limiters. A wide range of numerical schemes contains more or less traditional schemes, like the upwind scheme and Lax-Friedrichs scheme (first order) or Lax-Wendroff scheme

(second order). Some relatively new, popular and efficient schemes are TVD schemes or ENO schemes. New but not so frequent are composite schemes ([7–9]) or schemes using some filter to eliminate oscillations near shock waves. When somebody wants to find some details about higher order upwind or central schemes for 1D scalar equation or 1D system of Euler equations see *e.g.* [10]. For symmetric TVD schemes or some simplified TVD schemes see *e.g.* [11].

The 2D and 3D models of Euler equations have to be used in real numerical simulation. In multidimensional case nobody is still able to prove that scheme is TVD. Commonly a proper multi-dimensional extension of a 1D TVD scheme is used without theoretical background, but on the other hand the achieved results often showed similar quality of numerical solution like for the 1D problem (accuracy, not oscillated result near the shock wave, proper motion of the shock wave, ...). When one uses as a governing system the multi-dimensional system of Navier-Stokes equations, the convective part is usually approximated by multi-dimensional extension of the mentioned schemes and dissipative part by central differencing using some type of approximation (*e.g.* auxiliary finite volumes).

Our group followed trends described above and during last years developed several 2D and 3D methods for computation of transonic flows in internal and external aerodynamics based on following schemes (finite volume methods):

a) older version of Mac Cormack scheme and two TVD versions of Mac Cormack scheme (simplified and full version [12, 13]),
b) cell vertex Ron-Ho-Ni scheme [14],
c) several TVD upwind schemes based on MUSCL interpolations and then approximative Riemann solver or Lax-Friedrichs flux [15, 16],
d) TVD implicit scheme based on first order preconditioning and Osher method [17],
e) ENO and WENO method [8],
f) composite scheme on basic triangular grid and dual grid (predictor-corrector scheme) in cell vertex form 2D, 3D [9],
g) Runge-Kutta multistage scheme based on the idea of Jameson, Turkel and Schmidt.

All mentioned schemes have been commonly tested not only for simple cases, but also for more complicated physical and engineering problems. Some results achieved in several tests will be mentioned in the next section. The results show accuracy of the method, properties of artificial viscosity terms, properties of grid used in solution, and so on.

4. Some numerical examples of transonic flow

We developed several tests of 2D transonic flows. The first test case is the inviscid steady transonic flows in the so-called GAMM channel (see Figures 4 and 5) with $M_\infty = 0.675$ and bump of 10% (one half of 20% DCA symmetrical airfoil). The well known feature (computation) is $\max M \approx 1.37 - 1.38$, as well as the location of a shock wave and appearance of the so-called Zierep singularity behind the shock wave when one considers the distribution of Mach number along the wall with a bump (lower wall). Figure 4 shows a numerical solution in the form of Mach number

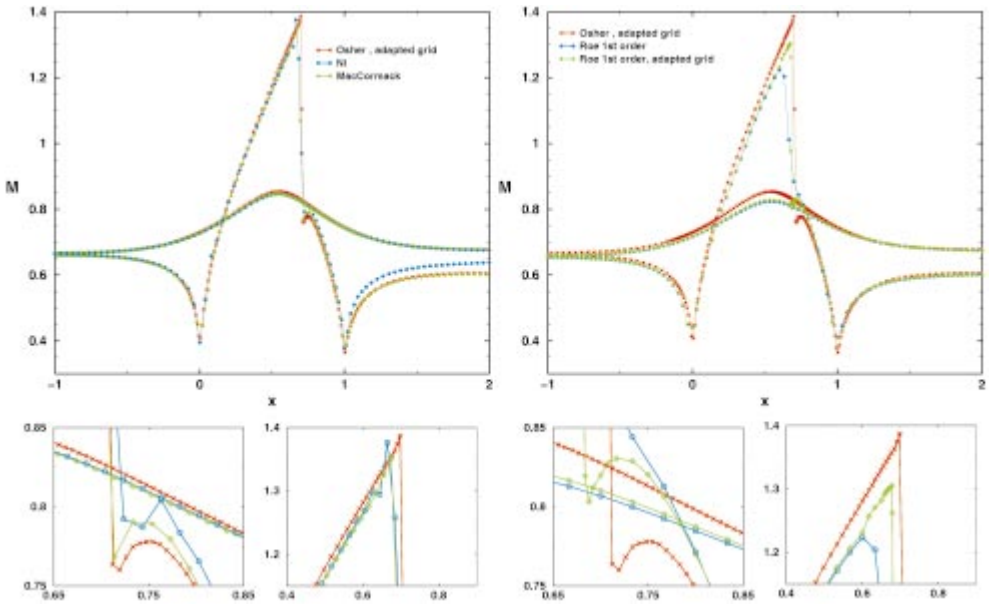

Figure 4. GAMM channel: distribution of M along walls and details near upper and lower part of shock wave

distribution on the walls (lower, upper) computed by several developed methods, Figure 5 shows results in the form of iso-Mach lines only for two computed cases, because the picture of results using isolines is very similar for all results. Results achieved by a higher order Osher scheme with WENO reconstruction on an adapted grid are used as reference values on both left and right parts of Figure 4, details of main graphs near the upper and lower part of the shock wave are located below each part. Results achieved by central type schemes on a structured grid are plotted in the left part. We can observe that these methods without any grid adaptation reach the expected maximum of Mach number in front of the shock wave. The method with a TVD type of artificial viscosity term does not produce any oscillations and maps more correctly the region of Zierep singularity than the method with Jameson's type of artificial viscosity. The right part compares results achieved by upwind schemes of second (reference) and first order with and without adaptation. One can observe that the first order method (modified Roe scheme) cannot reach the expected maximum of Mach number. Several steps of grid adaptation can increase the maximum of Mach number, and presence of the Zierep singularity is observed. We can mention that the

Figure 5. GAMM channel: Iso-Mach lines; TVD MC (left), Osher implicit method on adapted grid (right)

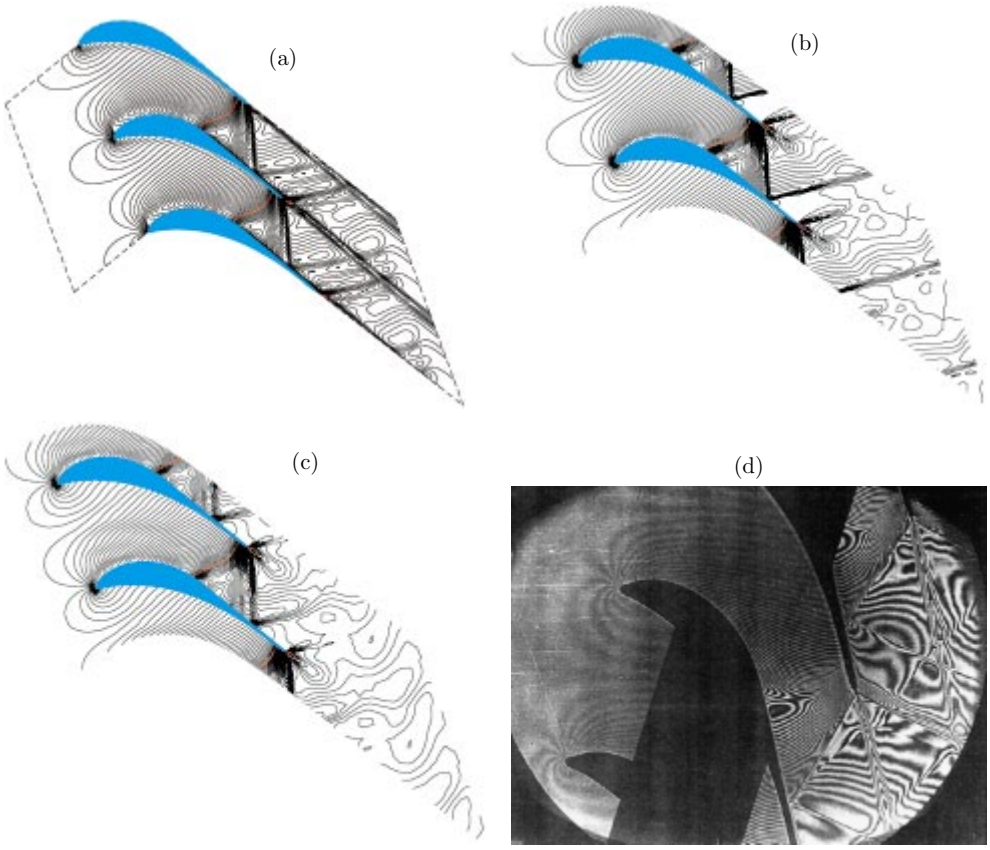

Figure 6. Turbine cascade SE1050: Iso-lines of Mach number and experiment – strips of constant density; (a) TVD Osher scheme, H type grid (b) TVD Osher scheme, adapted triangular grid (c) TVD Roe scheme, adapted triangular grid (d) interferogram of IT CAS

higher order version of the method (MUSCL reconstruction) with grid adaptation yields a result very similar to the reference one.

The second test case is inviscid steady transonic flow through an SE1050 turbine cascade measured by IT CAS (interferometric measurements). The main features of flow are: subsonic inlet, transonic outlet ($M_{2_{is}} \simeq 1.198$), compression domain in the second part of the channel between the blades, closed sonic line, structure of shock waves and reflected shock waves in the downstream part of the flow field. Figure 6a shows numerical results using iso-Mach lines computed by the implicit TVD method and H-type grid, Figure 6b – using the same method but on a triangular grid with adaptation, and Figure 6c – computed by the explicit TVD method (Roe) in the form of Mach number isolines. It is possible to compare all achieved results with experimental interferometric data of IT CAS shown in Figure 6d. The H-type grid of quadrilaterals does not capture correctly the profile geometry near the leading edge and therefore one can see the influence of entropy production in a layer near the suction side of the profile and behind the trailing edge – like a wake (Figure 6a). This phenomenon is effectively suppressed by an adaptive triangular grid (Figure 6b, c).

We can also see that the left running shock wave is captured better on a quadrilateral (Figure 6a) than on triangular grid independent of the type of upwind scheme.

The third test case is transonic flow through a DCA 8% cascade of IT CAS computed for inviscid flow and also for laminar viscous flow. This viscous test case is more academic than real, but can show strong influence of artificial viscosity effects in computation of viscous flows. We consider $\mathrm{Re} = 6\,450$ and $M_\infty = 0.76$, $\alpha = 2^\circ$. The first numerical results of this case were achieved by [18] and multistage Runge-Kutta methods. The flow was computed as steady flow. Our results were achieved later by the TVD Mac Cormack method (or not far from TVD) and by WENO scheme of high order. These results plotted in a form of iso-Mach lines show unsteady regimes and for the same time T one can compare results achieved by different methods. Both methods are less dissipative than the Runge-Kutta method and WENO is less dissipative than the Mac Cormack method. Both methods achieved an unsteady solution with a Kárman vortex street in the wake, see Figure 7, 8, and confirmed that our older results achieved by the multistage RK method [18] were not very accurate!

Figure 7. WENO scheme, 50 000 time steps (left), 50 200 time steps (right)

Figure 8. TVD Mac Cormack scheme, 50 000 time steps (left), 50 200 time steps (right)

The next test case is 3D transonic flow through a turbine cascade of Škoda Pilsen. Transonic flow through the stator and rotor blade row has been computed by the cell centered (TVD Mac Cormack scheme) and cell vertex (modified Ni scheme) schemes on the same relatively simple H type grid. Outlet flow parameters computed for the stator blade were recomputed into the relative frame of reference and have been used (in proper form) as inlet parameters for computation of flow through the rotor blade row. Figure 9 compares results of both methods for the stator, Figure 10 for the rotor blade row in the case when body forces were not taken into account. Both results are plotted in a form of iso-Mach lines for several cross-sections in different positions in the span-wise direction.

We can generally observe a good agreement between the results achieved by both methods. Some differences are in the mapping of the shock wave structure in the cross-section of the stator blade near the hub, results differ a little bit more for the highly twisted long rotor blade of the low pressure turbine stage. The next figure (Figure 11a) also shows a very good agreement of the computed radial distribution of inlet and outlet parameters for the rotor blade. Figure 11b shows a significant redistribution of inlet flow parameters (near the hub) for the case when body forces are

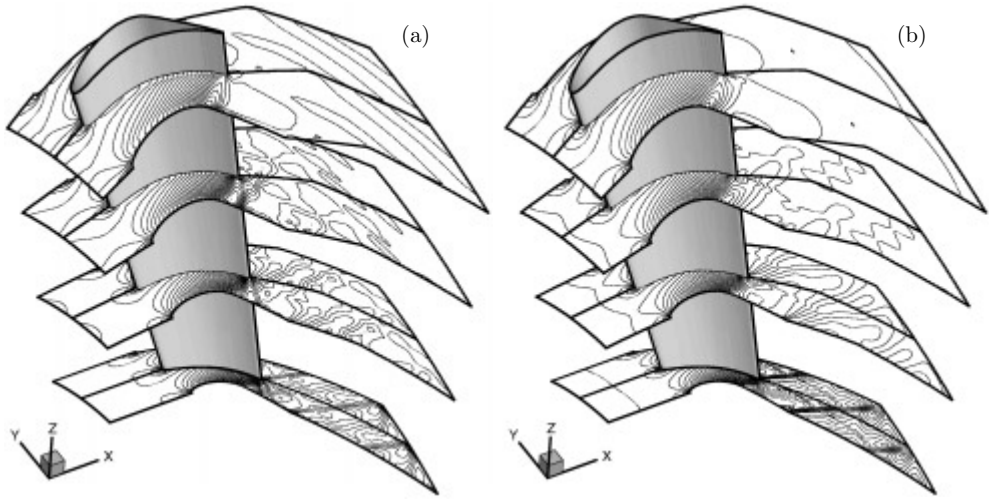

Figure 9. 3D stator axial turbine blade row: Iso-Mach lines;
(a) TVD MacCormack scheme, (b) Ni's scheme

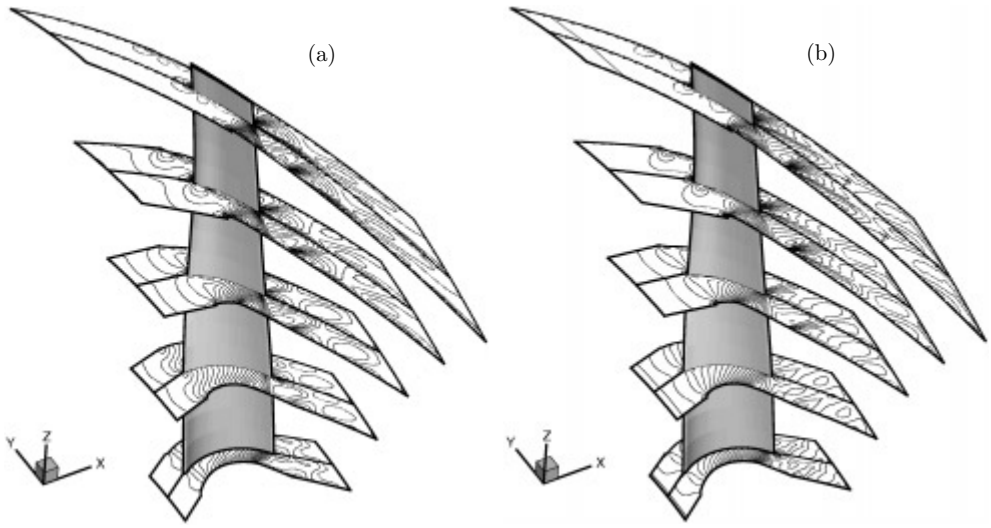

Figure 10. 3D rotor axial turbine blade row; Iso-Mach lines;
(a) TVD MacCormack scheme, (b) Ni's scheme

considered. Both methods use central Lax-Wendroff type schemes of second order. To achieve the presented agreement of results is not so simple for such complex industrial problems. It needs proper mathematical formulation of boundary conditions, grid, parameters of the method (*e.g.* coefficients in artificial viscosity terms). Comparisons of results achieved by independent methods (it means different *e.g.* grid, scheme and artificial viscosity, finite volume, approximation of boundary conditions) are necessary for validation of results of numerical simulations used for industrial purposes especially in cases when experimental data are not available.

The next figure compares results of transonic flow for the radial stator turbine cascade computed by the method of first order (Roe type Riemann solver) and higher

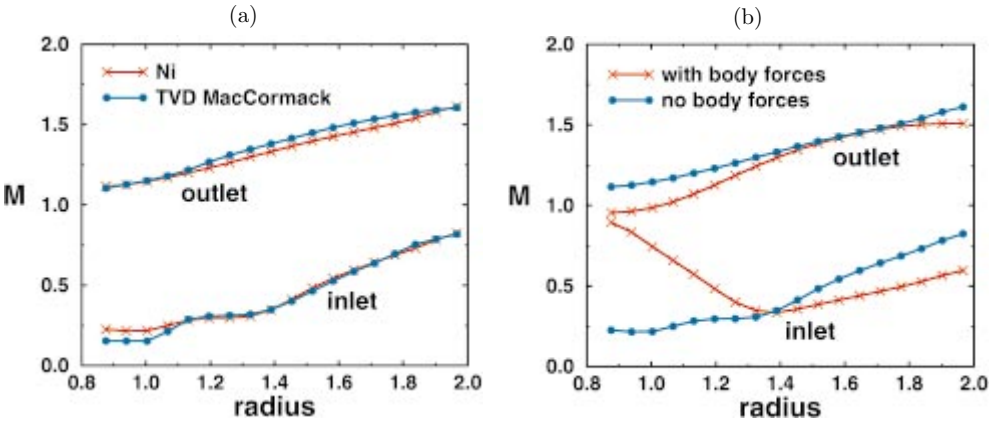

Figure 11. 3D rotor blade; (a) inlet and outlet Mach number distribution, (b) inlet and outlet Mach number distribution

order method (Osher Riemann solver, WENO reconstruction) on a triangular grid (iso-Mach lines). The main features of transonic flow through this cascade are the significant acceleration of flow in the downstream direction and strong shock waves crossing the outlet part. We can see a very good agreement of the computed results in Figure 12a, b although the first method is higher order and the second one only first order. The pressure distribution along the profile surface shows that the influence of the grid near the leading and trailing edges (Ni scheme has been used on an H type grid) is more important than the numerical scheme in this case.

5. Turbulent flows

There are several ways to compute turbulent flows:

a) mostly preferred RANS equations (Reynolds Averaged Navier-Stokes equations) in the laminar (formally) form (or modified at the right hand side by some additional terms or source terms) and some special way to compute the so-called turbulent viscosity coefficient,
b) RANS equations and for micro-turbulent structure LES in the form the Smagorinsky model,
c) DNS for some special forms of turbulent flows or to investigate the transitional part between laminar and turbulent flows.

We prefer at our group now mainly part a) and we have some experience with part b). In part a) mainly algebraic, one-equation, two-equation and RSM (simplified) models are used to compute turbulent flows. More frequent models are:

α) algebraic:
- Baldwin-Lomax,
- Johnson-King,
- some RNG versions,

β) among one-equation models mainly the Spalart-Almaras model,
γ) among two-equation models k-ε, k-ω or some modifications of the mentioned models. Recently, the SST model of Menter [19] seems to be very successful.

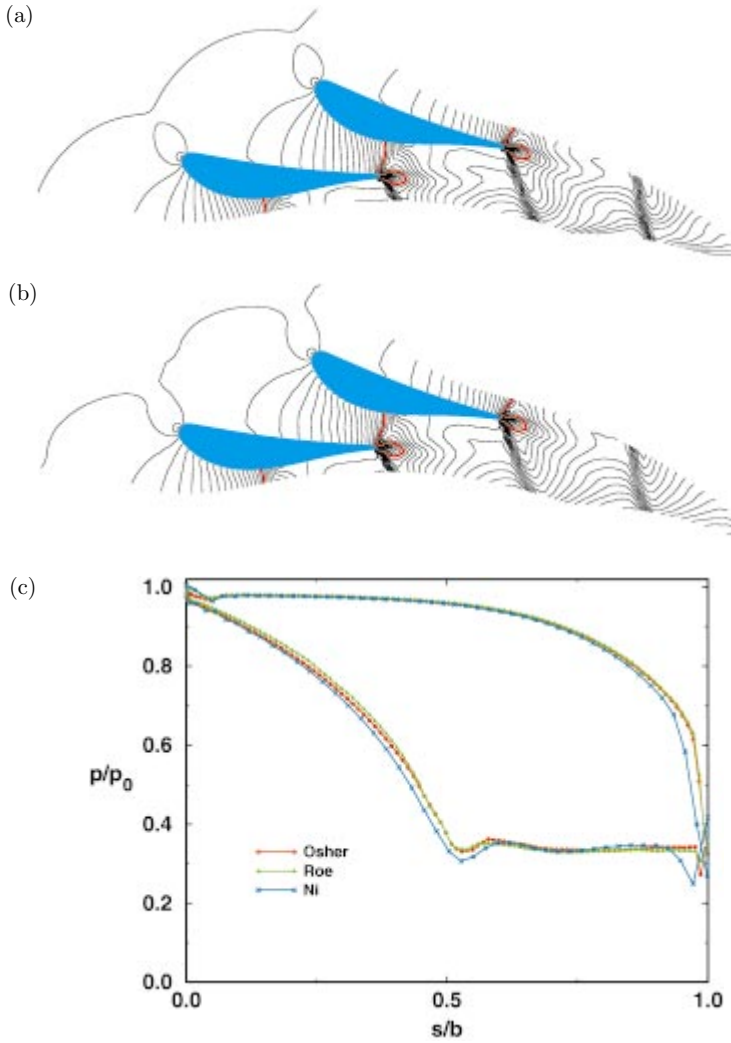

Figure 12. Turbine radial stator cascade: (a) Osher scheme, WENO reconstruction, (b) first order Roe scheme, (c) Pressure distribution along profile

We have an experience (numerical) with the Baldwin-Lomax model and two-equation model (k-ω) for 2D transonic flows in external aerodynamics. Another part of our group has an experience with several two-equation models (k-ε, k-ω), see Figure 14, for 2D and 3D incompressible turbulent flows. Recently, the best results have been achieved with Menter's SST model [19].

We have developed several numerical methods (2D and 3D) [20, 21] computing the incompressible viscous (laminar or turbulent) flow based on:

a) Mac Cormack scheme,
b) RK-multi stage scheme,
c) Crank-Nicholson (CN) and some modification of CN scheme,
d) AUSM scheme,
d) Kuwahara modified scheme.

The last two schemes have high accuracy, order ≥ 3 for convective terms (3^{rd}, 5^{th} order) and order ≥ 2 for dissipative terms (2^{nd}, 4^{th}, 6^{th} order).

Figures 13 and 14 compare computed results of 2D incompressible impinging jet flows (IJF) for a 2D ERCOFTAC case achieved by several turbulence models. Figure 15, 16 show 3D results for $\text{Re} = 23\,000$ (turbulent).

Figure 13. Isolines of velocity for 2D jet, linear (left) and non-linear (right) SST model

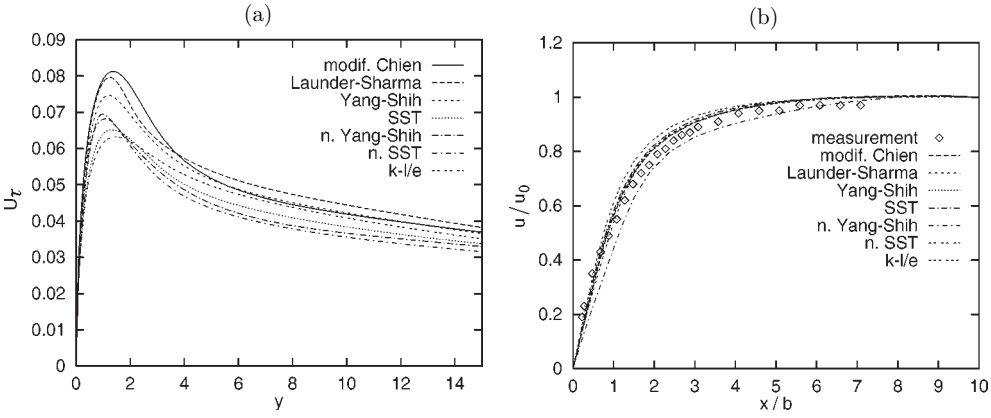

Figure 14. 2D impinging jet: (a) friction velocity, (b) velocity on jet axis

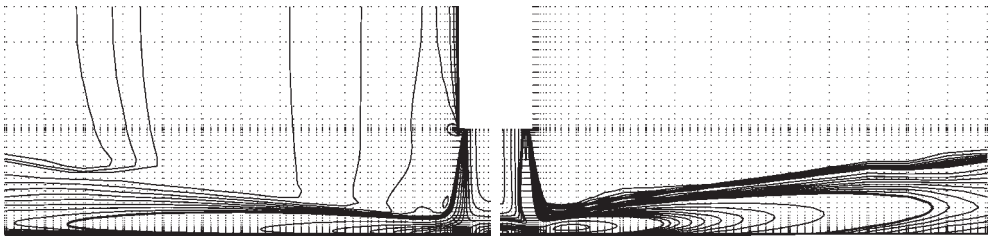

Figure 15. 3D impinging jet: isolines of velocity (left) and of k (right)

Figure 17, 18 show the computation of a turbulent case of backward facing step flows (BFS) for $\text{Re} = 13\,333$. Figure 17 then shows details of the computed results near the corner.

Using some examples, we showed that numerical simulation can be successful only if one uses:

a) suitable mathematical and physical model (including turbulence modelling),
b) suitable mesh appropriate for the geometry of the solved problem and scheme (with second or higher order accuracy) that is chosen sufficiently dissipative, but not too much for the case of high Reynolds number flow,

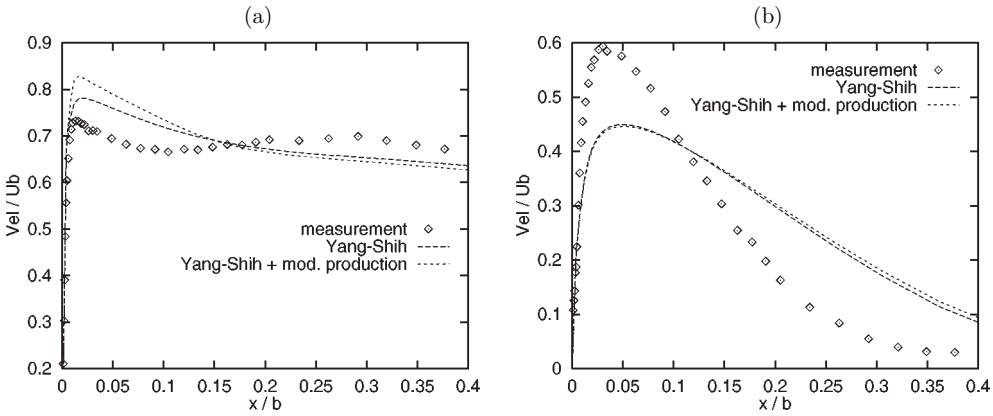

Figure 16. 3D impinging jet: (a) $r/D = 0.5$, (b) $r/D = 2.5$

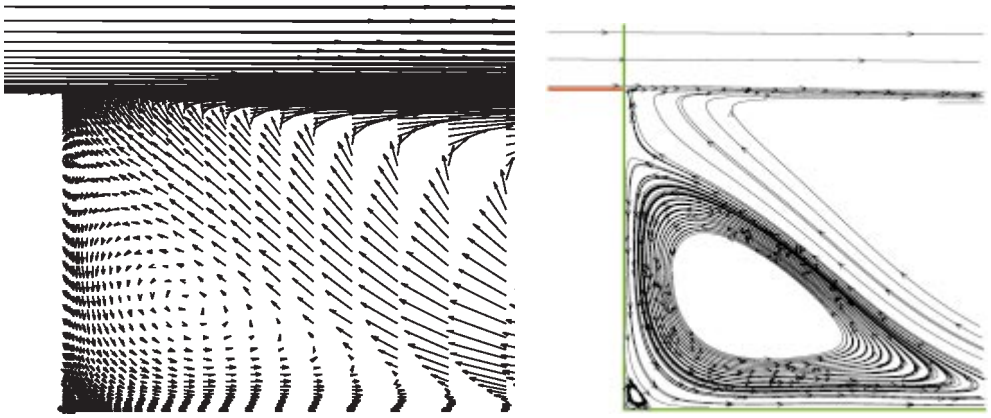

Figure 17. Flow field behind the step: velocity vectors and streamlines; Re = 13 333

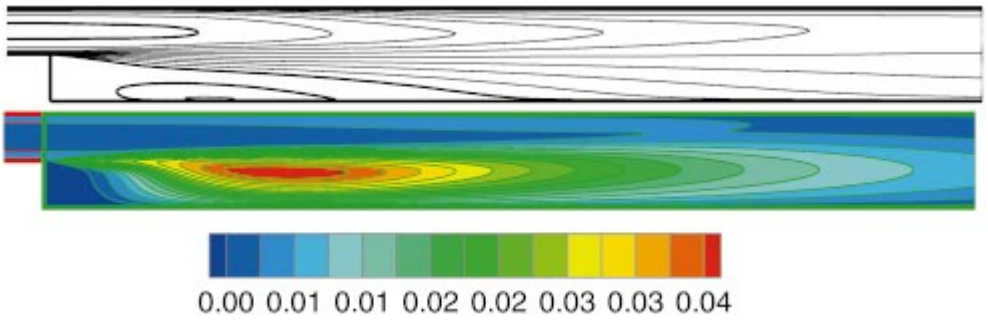

Figure 18. Isolines of velocity (above) and turbulent kinetic energy (below) in 2D, Re = 13 333

c) suitable and sufficiently accurate results with the examined rate of convergence or compared to experimental or other numerical results or analytical results. In this case adaptation of the grid and multi-grid solution is very often used.

We do not know the best schemes or turbulent models or grids. It is possible to mention more or less suitable schemes or turbulent models for a given case of flow and

geometry. We can say that mainly the recently published schemes 'not far' from TVD schemes (ENO, WENO, RK, ...) or not very dissipative TVD schemes are commonly used in numerical simulation with sufficient success.

6. Closure

The development of numerical methods at CTU Prague and IT CAS CR is shortly described mainly for transonic flows in internal aerodynamics. Then some commonly used mathematical models and numerical methods mainly based on the system of Euler and shortly on the system of Navier-Stokes equations were described. We deal more with numerical approximation of the convective part of the equations for high upstream velocity (high Reynolds number) than with the dissipative part. We mentioned TVD, ENO, composite and other schemes for a relatively general finite difference and finite volume mesh (structured, unstructured, adaptive) in several examples of 2D and 3D transonic flows. Also some numerical results of turbulent flow were mentioned and presented.

The paper shows that the numerical solution realized at modern and efficient computers, carefully using modern as well as traditional schemes (taking into account the influence of grid, scheme, adaptation, turbulence model...), is at this time a very strong tool to find main properties of the flow. Numerical solution is also helpful for modern design in turbomachinery. Not only experimental and theoretical research seems to be a strong support in turbomachinery but also numerical simulation, as some application of mathematics, numerical mathematics, engineering and physical sciences is now a more and more important part of design of new modern aircrafts, turbines, power plants, *etc.* Theory as well as experimental and numerical research are now means to continue progress and better description of fluid flow problems.

Acknowledgements

This work has been supported by grants of the Grant Agency CR 101/98/K001, 101/00/1057 and Research Plans of MSM of the Czech Republic No. 210000003, 212200009.

References

[1] Cole J D and Murman E M 1971 *AIAA J.* **9** (1) 114
[2] Magnus R and Yoshihara H 1970 *AIAA J.* **8** (12) 1710
[3] Kozel K, Polášek J and Vavřincová M 1978 *Strojnický časopis* **2** 243
[4] Kozel K, Polášek J and Vavřincová M 1978 *Proc. 6th Int. Conf. Numerical Methods in Fluid Dynamics*, Springer-Verlag, pp. 405–409
[5] Cockburn B, Hou S and Shu C W 1990 *Math. Comp.* **54** 545
[6] Dolejší V and Feistauer M 2001 *Proc. Sem. Euler and Navier-Stokes Equations*, Prague, Czech Republic, pp. 31–34
[7] Kozel K and Fürst J 1995 *Proc. Conf. Numerical Modelling in Continuum Mechanics*, Prague, Czech Republic, pp. 103–112
[8] Kozel K, Angot P and Fürst J 1996 *Proc. Conf. Finite Volumes for Complex Applications*, Rouen, France, pp. 283–290
[9] Kozel K, Janda M and Liska R 2000 *Proc. Conf. Hyperbolic Problems*, Magdeburg, Germany
[10] Yee H C 1989 *NASA Rep.* **101088** NANA Moffet Field, USA
[11] Yee H C 1987 *J. Comput. Phys.* **68** (1) 71
[12] Fürst J and Kozel K 2001 *Mathematica Bohemica Journal* **126** (2) 379

[13] Fořt J, Fürst J, Halama J and Kozel K 2001 *Mathematica Bohemica Journal* **126** (2) 354
[14] Fořt J, Fürst J, Halama J and Kozel K 2000 *Proc. IMACS Congress*, Lausanne, Switzerland
[15] Dobeš J, Fořt J, Fürst J and Kozel K 2001 *Proc. Sem. Topical Problems of Fluid Mechanics*, Prague, Czech Republic, pp. 33–36
[16] Kozel K, Fürst J, Horák J and Vaněk D 1999 *Proc. Sem. Topical Problems of Fluid Mechanics*, Prague, Czech Republic, pp. 19–22
[17] Fürst J and Kozel K *Proc. Sem. Navier-Stokes Equations: Theory and Numerical Solution, Research in Mathematics*, Series **388** 264
[18] Hůlek T, Huněk M and Kozel K 1992 *Proc. 1st European Computational Fluid Dynamics Conf.*, Brussels, Belgium, Vol. **1**, pp. 61–68
[19] Menter F R 1994 *AIAA J.* **32** (8) 1598
[20] Kozel K, Louda P and Příhoda J 2000 *Proc. IMACS World Congress*, Laussane, Switzerland
[21] Kozel K, Louda P and Příhoda J 2001 *Proc. GAMM Workshop Discrete Modelling and Discrete Algorithms in Continuum Mechanics*, ed. Sonar T, Logos Verlag, Berlin, pp. 157–166